Spin dynamics study and experimental realization of tunable single-ion anisotropy in multiferroic $Ba_2CoGe_2O_7$ under external magnetic fields

Rajesh Dutta,[1,2,*] Henrik Thoma,[1,2] Igor Radelytskyi,[2] Astrid Schneidewind,[2] Vilmos Kocsis,[3,4] Yusuke Tokunaga,[3,5] Yasujiro Taguchi,[3] Yoshinori Tokura,[3,6,7] and Vladimir Hutanu[1,2]

[1] *Institut für Kristallographie, RWTH Aachen Universität, 52066 Aachen, Germany*
[2] *Jülich Centre for Neutron Science at Heinz Maier-Leibnitz Zentrum, 85747 Garching, Germany*
[3] *RIKEN Center for Emergent Matter Science (CEMS), Wako, Saitama 351-0198, Japan*
[4] *Department of Physics, Budapest University of Technology and Economics, and MTA-BME Lendület Magneto-optical Spectroscopy Research Group, 1111 Budapest, Hungary*[†]
[5] *Department of Advanced Materials Science, University of Tokyo, Kashiwa 277-8561, Japan*
[6] *Quantum-Phase Electronics Center, Department of Applied Physics, University of Tokyo, Tokyo 113-8656, Japan*
[7] *Department of Applied Physics, University of Tokyo, Hongo, Tokyo 113-8656, Japan*

We report a spin wave study on multiferroic $Ba_2CoGe_2O_7$ under magnetic fields up to 12 T using low-energy inelastic neutron scattering. In-plane transverse (T_1) spin wave modes are highly dispersive along (h00) and rather flat but strong in intensity along (30l). In addition two dispersive electromagnon modes have been observed around 3.5 meV. Dispersion of the out-of-plane transverse modes (T_2) under fields reveals that the single-ion anisotropy constant decreases with increasing magnetic field which is consisted with the linear spin wave theory. Our results imply that the field dependent single-ion anisotropy plays a crucial role in determining the characteristics of T_2 and electromagnon modes in the three-dimensional anisotropic spin wave spectrum.

Strongly correlated electron systems involving square lattice Heisenberg antiferromagnets (SLHAF) with spin $\geq 1/2$ serve as an upstanding platform for studying many exotic quantum phenomena both experimentally and theoretically [1–6]. Emergence of exotic novel quantum phases, under external stimuli e.g. magnetic or electric field and uniaxial pressure or topological surface effect, are highly intercorrelated depending on the symmetric exchange, single-ion anisotropy (SIA) and Dzyaloshinskii-Moriya (DM) interactions [4, 7–12]. Multiferroic $Ba_2CoGe_2O_7$ is one of the intriguing quantum materials exhibiting induced spontaneous electric polarization which was explained by spin-dependent *d-p* hybridization mechanism [13–16], but in collinear staggered antiferromagnetic (AFM) state below the Néel temperature (T_N = 6.7 K). As a consequence both electro- and magnetic-active excitations (electromagnon modes) are expected in the multiferroics state and have been observed around 4 meV in the magnetic excitation spectrum along with conventional magnons using THz spectroscopy and inelastic neutron scattering (INS) [17–21].

However, the detailed information about the momentum resolved scattering cross sections S(Q,w) of the spin wave modes were not possible to obtain using ESR, FIR and circular dichroism THz spectroscopies as they can only probe the zone-center excitations in reciprocal space like Raman spectroscopy. Also, the previous INS studies on $Ba_2CoGe_2O_7$ [17, 19, 20] have dealt with only in-plane (*a*-*b*) spin dispersion where the applied magnetic fields were limited to 3 T, even far below the field (H $\approx$ 15 T) of onset saturation magnetization. In the presence of weak inter-plane ferromagnetic (FM) exchange interaction, $Ba_2CoGe_2O_7$ has been treated so far as quasi-two-dimensional (Q2D) AFM, but there is no single report on spin dispersion along *l*. As the induced electric polarization can be tuned by an external magnetic field, it is crucial to study the nature of the electromagnons as well the conventional magnons at relatively high fields in three-dimension, especially, when the system exhibits an effective spin anisotropy i.e. a strong intercorrelation between antisymmetric DM interactions and the SIA under the applied fields. Such interplay especially between the SIA and the magnetic field has remain hitherto unexplored through experimental findings in multiferroic quantum materials.

In this Letter, we present a detailed INS study on $Ba_2CoGe_2O_7$ under transverse magnetic fields up to 12 T at 4 K and reveal for the first time the tunable SIA constant under magnetic fields and the three-dimensional anisotropic nature of spin dispersion. We find that in-plane transverse modes (T_1) of magnetic *l*-dispersion are stronger than that along *h*-dispersion indicating the anisotropic in-plane spin fluctuations. The relatively high energy electromagnon modes (between 2.5 - 4.5 meV) are seemingly dispersive also in 3D, but slightly robust in the lower magnetic field region. Most interestingly, our findings on small changes in the SIA constant under magnetic field indicate that a competition between SIA and Zeeman interaction (external magnetic field) takes place when the SIA is quite strong in collinear state, thus providing a novel insight into general 2D square lattice AFM in the quantum limit.

INS experiment on a single crystal of $Ba_2CoGe_2O_7$ grown by the floating zone method [13, 14, 22, 23], was carried out on the cold-neutron triple-axis spectrometer PANDA at Heinz Maier-Leibnitz Zentrum (MLZ) [24]. The sample was aligned with its reciprocal ($h0l$) plane as horizontal scattering plane. Magnetic fields up to 12 T, using an actively shielded vertical cryo-magnet, were applied parallel to the vertical *b*-axis. The measurements were performed using a fixed final energy E_f = 5.107 meV of neutrons and the energy resolution at the elastic line was $\approx$ 0.16 meV. The incident and final energy were selected via the (002) Bragg reflection of pyrolithic graphite (PG) monochromator and analyzer with double focusing. A cooled Be filter was mounted before the analyzer to suppress the higher order neutrons. As shown

* Corresponding author: rajesh.dutta@frm2.tum.de
† *Present address*: *Institut fr Festkrperforschung, Leibniz IFW Dresden, 01069 Dresden, Germany*

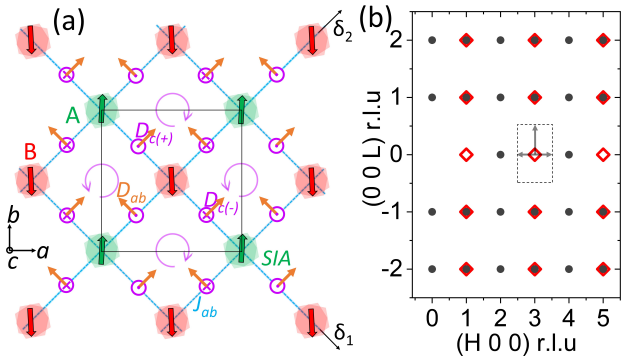

FIG. 1. (a) $Ba_2CoGe_2O_7$ unit cell (black square) projected along c-axis, only the Co^{2+} spins are shown in the sublattices A (green) and B (red) with the in-plane exchange interaction J_{ab} and DM interaction. On each bond along the direction i- to j-site indicated by δ_1 and δ_2. Staggered out-of-plane components of DM interaction $D_{c(+,-)}$ are represented as dotted and crossed pink circles respectively. Uniform components D_{ab} are shown as orange arrows. Colored filled double hexagons on each Co^{2+} indicates the on-site SIA. (b) Schematic of $(h0l)$ reciprocal plane containing both the nuclear (grey dots) and the magnetic (red empty diamonds) reflections. Black dotted rectangle indicates the magnetic Brillouin Zone of (300) where the arrows show the positions of performed constant-Q scans.

in Fig. 1, we interpret our results in the orthogonally twinned around c-axis and non-centrosymmetric tetragonal cell ($P\bar{4}2_1m$, lattice parameters $a = b = 8.41$ Å and $c = 5.537$ Å) [13, 20, 22], with the magnetic wave vector $\mathbf{q} = (1, 0, 0)$.

Figure 2 summarizes the effects of low-magnetic-fields on the three-dimensional magnetic excitations. Along both in- and out-of-plane directions, all the constant-Q scans show conventional T_1 and T_2 modes below 2.5 meV in energy and the weak electromagnon (EM) modes above 2.5 meV. Figure 2(b,d) explicitly shows that at zero-field both the maximum energy and the spin wave velocity (slope) of the T_1 mode along $(30l)$ are around five times less than that of T_1 mode along $(h00)$, which indicates the anisotropic nature of the 3D spin dispersion in $Ba_2CoGe_2O_7$. Please note that the intensity of the T_1 mode along the l-direction is ≈ 10 times the T_2 mode when $h = odd$ (see Fig. 2(c,d,g,h)) and it should be ≈ 0.1 times when $h = even$ confirmed by our calculation based on linear spin wave theory (LSWT). Nonetheless, an interesting feature is that the T_1 mode along l is more stronger than the T_1 mode along h which suggests the transverse in-plane spin fluctuations along l- and h-directions are anisotropic too. Here, the (T_2) mode is actually largely gapped mode (~ 2.25 meV) due to the strong SIA effect.

We have validated the observed conventional magnon modes in $Ba_2CoGe_2O_7$ under magnetic fields using the LSWT based calculation via SpinW code [25] considering a spin Hamiltonian given below,

$$\mathcal{H} = J\sum_{i,j}(S_i^xS_j^x + S_i^yS_j^y + \Delta S_i^zS_j^z) + J'\sum_{i,j}(\mathbf{S}_i\cdot\mathbf{S}_j) + \Lambda\sum_i(S_i^z)^2 + \sum_{i,j}\mathbf{D}_{i,j}\cdot(\mathbf{S}_i\times\mathbf{S}_j) - \sum_i g\mu_B\mathbf{H}^{ex}\cdot\mathbf{S}_i, \quad (1)$$

where i,j denotes neighboring Co^{2+} spin pairs. Even though the first term in the Hamiltonian represents the

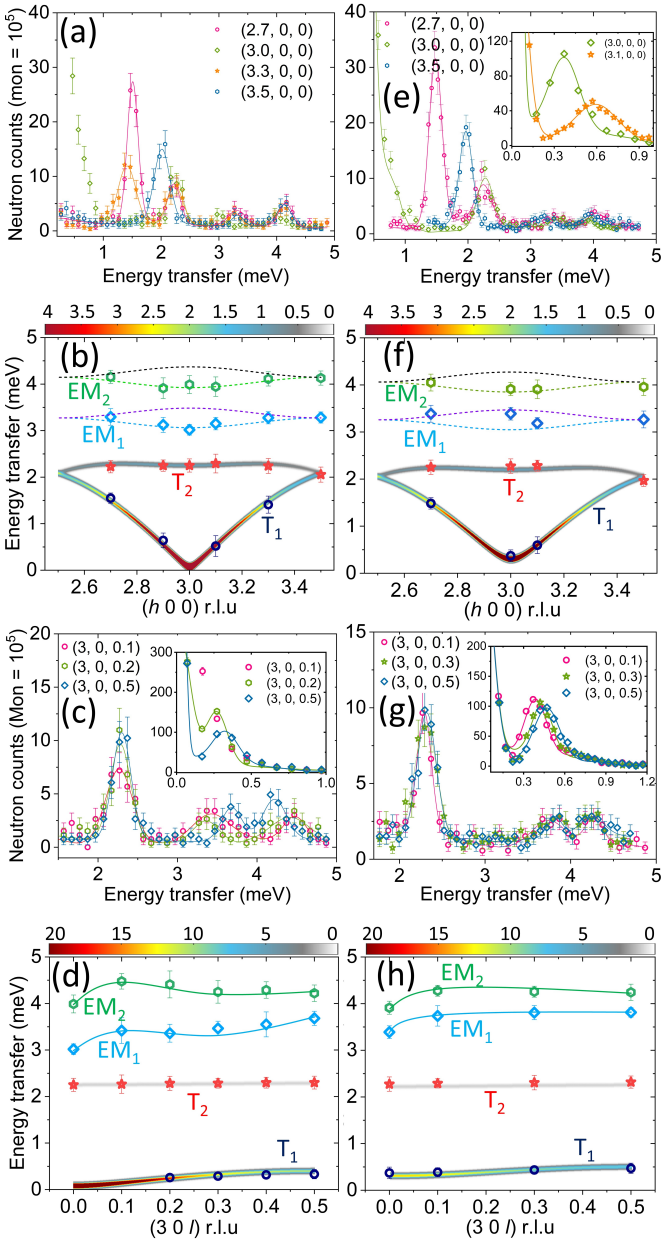

FIG. 2. Three-dimensional spin dispersion at magnetic fields of 0 T (left column) and 2 T (right column). (a,e) In-plane and (c,g) out-of-plane constant-Q scans and the corresponding calculated spin dispersion displayed in (b,f) and (d,h) respectively, with the overplotted dispersion points (ω, k). Only the solid lines in (d,h) are eye guide to the EM modes. The zoom sections in (e,c,g) represent the strong acoustic T_1 mode. All the vertical bars in (a-h) represents the corresponding error bars.

anisotropic Ising-type ($\Delta > 1$) exchange interaction but the leading axial easy-plane type SIA ($\Lambda \gg J\Delta$) term energetically favors the spin to lie on the a-b plane after competing with the DM interaction favoring a commensurate sublattice AFM ordering of the spins [20, 26]. While J' (< 0) is the weak FM interaction along the c-axis [15, 23]. The triple product represents the antisymmetric DM interaction and the last term is the Zeeman interaction. The staggered DM component in a closed loop (cl) inside the magnetic unit cell $\sum_{cl} D_{ij(c)} = 0$, indicated as circular arrows in Fig. 1(a) gives an unfrustrated condition of D_c but not for the D_{ab}. In the presence of a

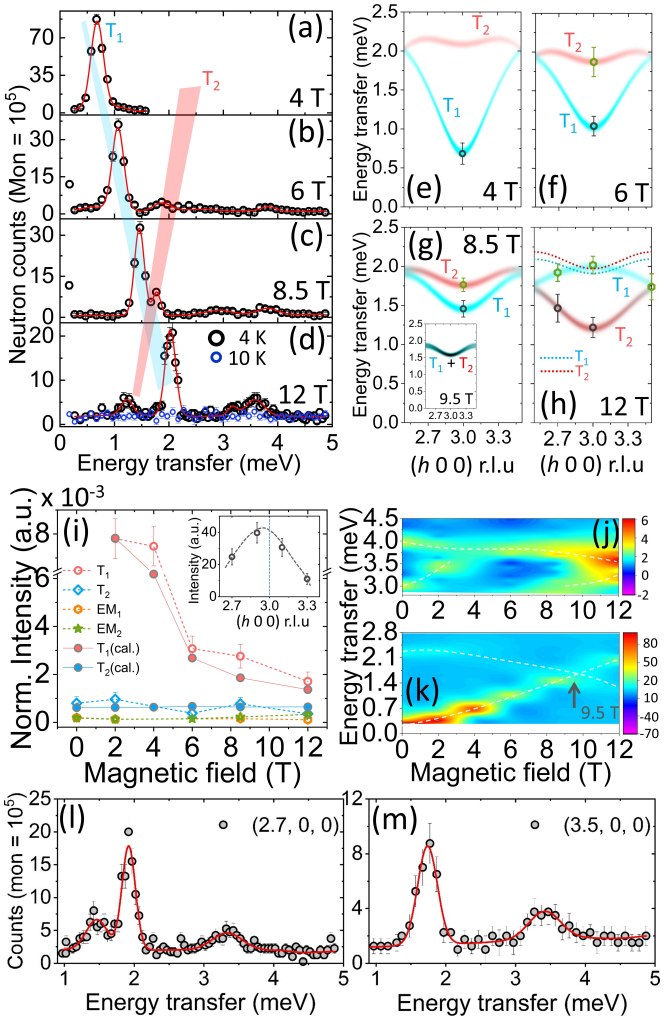

FIG. 3. (a-d) Zone center magnetic excitations at (300) under magnetic fields from 4 to 12 T at 4 K. Only the Bose factor correction was performed on the constant-Q scan at 10 K in (d) and the unit of the y-axis for this is $\chi^{''}$ in a.u. Highlighted red and lightcyan shedding correspond the T_1 and T_2 mode evolution with fields. (e-h) Shows the calculated spin dispersion overplotted with dynamical wave vectors under magnetic fields. Inset in (g) represent the calculated spin waves at 9.5 T. Only the dotted dispersion curve using the fixed SIA (0.75 meV) at 12 T has been overplotted in (h). (i) Intensities of T_1, T_2 and electromagnon ($EM_{1,2}$) modes at (300) under magnetic fields. (j,k) Contour plots of $EM_{1,2}$ and conventional magnon modes obtained from experimental constant-Q scans at (300) where arrow indicated the overlapped region and white dashes are eye guide to the modes. (l,m) Constant-Q scans at 12 T. All the vertical bars in (a-m) represents the corresponding error bars.

magnetic field (H^{ex}), the canting angle between the two sublattice spins is controlled by both the field and the DM interaction and the energy gap of the T_1 mode at the zone center depends mainly on the field strength as it dominates the U(1) explicit symmetry breaking, see Fig. 2(e-h). All the scans presented in Fig. 2 were fitted with simple Gaussian peak profiles without any background subtraction and we have achieved an excellent agreement between the experimental observation and the calculation.

To directly observe the effects of the SIA under magnetic fields, low energy INS spectra at the AFM zone center (300) were measured up to 5 meV as shown in Fig. 3(a-d) along with the simulated dispersions in Fig. 3(e-h). With increasing field the gap of the T_1 (T_2) mode continue to increase (decrease) and finally getting overlapped at certain critical field (H_c). Both experimentally and theoretically we find $H_c \approx 9.5$ T (see Fig. 3(k) and inset of Fig. 3(g)). With further increasing field a complete mode crossing take place e.g. at H = 12 T (Fig. 3(d,h)). Most likely at $H_c \approx 9.5$ T the effective anisotropy is not strong enough to compete the Zeeman interaction and therefore, an anomaly in the magnetization curve occurs and also the induced c-component of electric polarization (P_c) starts to decrease at H_c which have been experimentally observed in Ref. [13–15]. We show next that such competition results in tunable SIA constant under fields. However, the obtained and calculated field dependent intensities (normalized w.r.t the magnetic Bragg peak) of the zone center modes are plotted in Fig. 3(i) with the inset showing typical Q-dependence intensity fall at 0 T.

Let us begin with the study on the unconventional EM modes under fields. The zone center electromagnon ($EM_{1,2}$) modes are plotted as a contour map in Fig. 3(j). For the first time, instead of so far reported one EM mode, we have observed two EM modes experimentally in the INS spectra. Also, such two EM modes have been predicted theoretically in Miyahara et al. [27] via an exact diagonalization on 12-site clusters calculation and in Romhányi et al. [28] via multiboson spin-wave theory. These EM modes are not captured by our LSWT calculation as the higher order spin interaction terms are not implemented. Nevertheless, to describe the dispersive nature of the EM modes under magnetic fields, we have used the solutions of the effective Hamiltonian proposed by Penc et al. [18] and Romhányi et al. [28] in the frame of a multiboson theory for the in-plane spin stretching modes in $Ba_2CoGe_2O_7$. Even though DM interactions were not included in the reported zero-field multiboson dispersion relations $\omega_{c,d}(k)$ for EM modes, we could almost explain the observed EM dispersive nature along (h00) after considering variable SIA constants and higher order terms (see the Fig. 4(a)). Only lower branches of $EM_{1,2}$ modes have been observed and they agree nicely with the calculated $\omega_{c,d}(k)$ dispersion relations. These EM modes are suggested to be sensitive to the spin stretching amplitude [18] and the equivalent d-p hybridized antiferroelectric constant i.e. spin nematic interaction [19]. Interestingly, we find that they are dependent on the SIA, in other words on the external magnetic fields as well. As shown in Fig. 4(a,b) the EM_1 modes seem to be quite robust at 0 and 2 T whilst at 12 T the EM_2 modes shift to the lower energy near the EM_1 mode. We believe that the changes in the SIA constant under fields is responsible for this phenomena since the antiferroelectric constant from the d-p hybridization coupling might be sensitive to applied electric and magnetic field via the crystal electric field (CEF) effect and also under external pressure [11].

To extract the strength of the exchange interactions (J = 0.207, J' = -0.0052 meV and Δ = 1.18); the DM interactions (D_{ab} = 0.015, D_c = ±0.0103 meV); the SIA constant ($\Lambda_{H=0}$ = 0.75 meV) we have performed the refinement of the INS spectrum using the SpinW code. Slight anisotropic g-tensors have been incorporated in the Hamiltonian at higher fields to adjust the gap in the T_1 mode. Similarly, after careful inspection of the energy

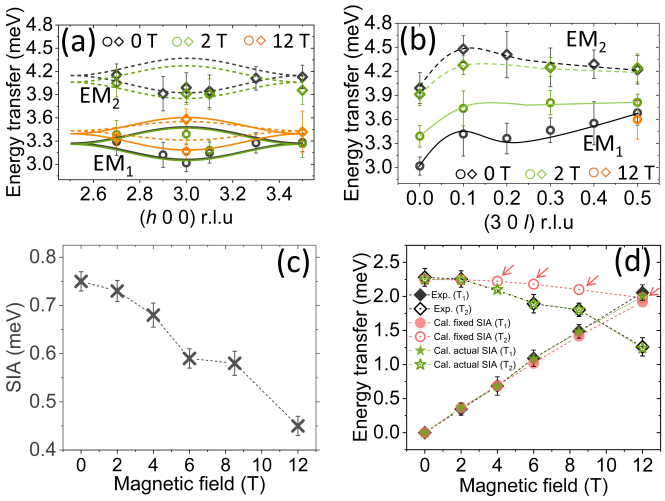

FIG. 4. Evolution of in-plane (a) and out-of-plane (b) electromagnon modes under magnetic fields. In (a) solid and dashed lines are calculated dispersion curves while in (b) they are guide lines (not calculated). Solid line and open circles corresponds to EM_1 mode while dashed line and open diamonds for EM_2 mode. (c) Values of SIA constants under external magnetic fields. (d) Energy values of magnetic field dependent T_1 and T_2 modes obtained via experiment and calculations; (black) experimentally observed, (red) calculated while keeping the zero-field SIA constant ($\Lambda = 0.75$ meV) fixed and (green) calculated using the actual SIA constants taken from (c). Red arrows indicates highly deviated T_2 modes (red open circles) from experimental (green open stars). All the vertical bars in (a-d) represents the corresponding error bars.

value of the T_2 mode at (300) presented in Fig. 2 and Fig. 3(a-h), we have noticed that the changes in its energy value are mainly depends on the changes in the SIA constant being independent of other interactions. Of course the SIA affects the T_2 mode over whole Q-range but most dominant change occurs at zone center (300) while these T_2 modes in the THz spectrum are barely visible to determine the SIA effect. It is worth to mention that the size of SIA constant in this present study at 4 K is slight smaller than the value reported in the studies [17, 19] at 1.5 K. The reason for this deviation could be the different measurement temperatures. Such decrease in SIA constant with temperature has been observed as well in other multiferroic antiferromagnets like $BiFeO_3$ [29] and $HoMnO_3$ [30]. However, the value of SIA constant and its effect mainly on T_2 mode under applied magnetic fields are presented in Fig. 4(c,d). The fixed value of zero-field SIA constant does not give a good agreement with the experimental observation for the fields above 2 T and it also shows the mode crossing take place at incorrect field near 12 T. We have confirmed via simulations that this change in energy level of T_2 can only be reproduced by varying the strength of the SIA constant not that of J or DM interaction. Since the difference between considering fixed or actual SIA is much more pronounced for the T_2 mode, we have presented the simulated dispersion curve with the fixed SIA in Fig. 3(h) and two extra constant-Q scans are shown in Fig. 3(l,m) to deliver the confidence on the calculation using actual SIA. Thus, we conclude that the SIA constant gets tuned under magnetic field and therefore effecting the T_2 and the EM modes which are remarkable and novel findings in the physics of multiferroic quantum SLHAF materials.

From the theoretical aspect, in the absence of DM interaction and field, AFM quantization axis is chosen arbitrarily where spontaneous rotational symmetry U(1) breaking gives rise to a Goldstone mode. But under applied magnetic field, the induced canting angle ($\delta\varphi$) between the sublattice spins in the magnetic ground state is not any more arbitrary keeping the order parameter (η) unchanged until the onset of saturation magnetization and give rise to a gap for T_1 mode. In the Hamiltonian Zeeman term is quite strong as SIA term e.g. a magnetic field of 6 T has same order of magnitude in energy ($g\mu_B H \approx 0.69$ meV) as SIA constant and a competition could take place between them since the transverse field itself forces the spins to be planner and quantized along its direction. On the other hands, magnetic field can mediate the magnetic anisotropy via CEF and spin-orbit coupling (SOC). In the $3d^n$ transition metal ions, CEF effects are stronger than SOC but a comparable SOC leaves the orbital moment unquenched and introduces an extra orbital splitting in addition to those CEF splitting modifying the magnetic anisotropy. Such unquenched orbital angular momentum [31] under rotations of magnetic field and also the toroidal moment [32] have been found in $Ba_2CoGe_2O_7$ which confirm the presence of SOC effect. Since the magnetic field induces a local electric field in the tetrahedral metal-ligand (CoO_4) environment (because of its multiferroic properties), CEF and SOC coupling both act accordingly with that and might results in tuning of the magnetic anisotropy. Such microscopic origin of the SIA changes could perhaps be better studied by means of detailed CEF excitations energy levels under magnetic fields and considering the CEF parameters and intermediate SOC coupling as perturbation into the effective Hamiltonian, allowing the precise determination of CEF parameters (B_n^m) and construction of detailed maps of magnetic and g-anisotropy to be studied.

In summary, our study reveals for the first time, three-dimensional anisotropic spin excitations in the multiferroic antiferromagnet $Ba_2CoGe_2O_7$, under applied magnetic fields up to 12 T at 4 K. In fact, contrast to conventional magnons, INS spectrum shows the existence of two unconventional electromagnon modes which are also disperive in 3D and responsive to the external magnetic field. Most strikingly, external magnetic field leads to a tunable axial easy-plane type SIA which is a remarkable finding as it also gives a hint to have possible similar effects in presence of external electric field. In particular, all the conventional spin wave modes under magnetic fields are in well accordance with the calculated spin dispersion via LSWT considering a spin-3/2 model Hamiltonian. Nevertheless, this study provides a novel insight to a complex intercorrelation among the SIA, the DM interaction and the external magnetic field in SLHAF materials leading to many interesting key features like mode crossing and anisotropy spin gap of T_1, T_2 modes. Our study encourages to search further for novel multiferroic devices where the tuning of SIA either via electric or magnetic field is possible and investigate the dynamical aspects where the SIA is less dominant and spins are non-collinear like in its sister compound $Ba_2Cu_{1-x}M_xGe_2O_7 (M = \text{Co, Mn})$.

ACKNOWLEDGMENTS

We thank Professor I. Kézsmárki for the fruitful discussions. We thank technician team for helping us with the cryo magnet at PANDA. R. D. and V. H. would like to acknowledge the support from Institut für Kristallographie, RWTH Aachen Universität and Jülich Centre for Neutron Science at Heinz Maier-Leibnitz Zentrum.

[1] S. Chakravarty, B. I. Halperin, and D. R. Nelson, Phys. Rev. B **39**, 2344 (1989).

[2] Z. Weihong, R. H. McKenzie, and R. R. P. Singh, Phys. Rev. B **59**, 14367 (1999).

[3] W. Selke, G. Bannasch, M. Holtscheider, I. P. McCulloch, D. Peters, and S. Wessel, Condensed Matter Physics **12**, 547 (2009).

[4] J. Romhányi, F. Pollmann, and K. Penc, Phys. Rev. B **84**, 184427 (2011).

[5] S. Kar, K. Wierschem, and P. Sengupta, Phys. Rev. B **96**, 045126 (2017).

[6] D. C. Johnston, Phys. Rev. B **95**, 094421 (2017).

[7] Z. L. Li, J. H. Yang, G. H. Chen, M.-H. Whangbo, H. J. Xiang, and X. G. Gong, Phys. Rev. B **85**, 054426 (2012).

[8] T. Goswami and A. Misra, Chemistry A European Journal **20**, 13951 (2014).

[9] P. Frbrich, P. Jensen, and P. Kuntz, The European Physical Journal B - Condensed Matter and Complex Systems **13**, 477 (2000).

[10] J. Romhányi, M. Lajkó, and K. Penc, Phys. Rev. B **84**, 224419 (2011).

[11] T. Nakajima, Y. Tokunaga, V. Kocsis, Y. Taguchi, Y. Tokura, and T.-. H. Arima, Phys. Rev. Lett. **114**, 067201 (2015).

[12] Z. L. Li, J. H. Yang, G. H. Chen, M.-H. Whangbo, H. J. Xiang, and X. G. Gong, Phys. Rev. B **85**, 054426 (2012).

[13] V. Hutanu, A. P. Sazonov, M. Meven, G. Roth, A. Gukasov, H. Murakawa, Y. Tokura, D. Szaller, S. Bordács, I. Kézsmárki, V. K. Guduru, L. C. J. M. Peters, U. Zeitler, J. Romhányi, and B. Náfrádi, Phys. Rev. B **89**, 064403 (2014).

[14] H. Murakawa, Y. Onose, S. Miyahara, N. Furukawa, and Y. Tokura, Phys. Rev. Lett. **105**, 137202 (2010).

[15] H. Murakawa, Y. Onose, S. Miyahara, N. Furukawa, and Y. Tokura, Phys. Rev. B **85**, 174106 (2012).

[16] M. Soda, S. Hayashida, B. Roessli, M. Månsson, J. S. White, M. Matsumoto, R. Shiina, and T. Masuda, Phys. Rev. B **94**, 094418 (2016).

[17] M. Soda, L.-. J. Chang, M. Matsumoto, V. O. Garlea, B. Roessli, J. S. White, H. Kawano-Furukawa, and T. Masuda, Phys. Rev. B **97**, 214437 (2018).

[18] K. Penc, J. Romhányi, T. Rõ om, U. Nagel, A. Antal, T. Fehér, A. Jánossy, H. Engelkamp, H. Murakawa, Y. Tokura, D. Szaller, S. Bordács, and I. Kézsmárki, Phys. Rev. Lett. **108**, 257203 (2012).

[19] M. Soda, M. Matsumoto, M. Månsson, S. Ohira-Kawamura, K. Nakajima, R. Shiina, and T. Masuda, Phys. Rev. Lett. **112**, 127205 (2014).

[20] A. Zheludev, T. Sato, T. Masuda, K. Uchinokura, G. Shirane, and B. Roessli, Phys. Rev. B **68**, 024428 (2003).

[21] S. Bordács, I. Kézsmárki, D. Szaller, L. Demkó, N. Kida, H. Murakawa, Y. Onose, R. Shimano, T. Rõ om, U. Nagel, S. Miyahara, N. Furukawa, and Y. Tokura, Nature Physics **8**, 734 (2012).

[22] V. Hutanu, A. Sazonov, H. Murakawa, Y. Tokura, B. Náfrádi, and D. Chernyshov, Phys. Rev. B **84**, 212101 (2011).

[23] V. Hutanu, A. Sazonov, M. Meven, H. Murakawa, Y. Tokura, S. Bordács, I. Kézsmárki, and B. Náfrádi, Phys. Rev. B **86**, 104401 (2012).

[24] A. Schneidewind and P. Čermák, Journal of large-scale research facilities, 1, A12 (2015).

[25] S. Toth and B. Lake, Journal of Physics: Condensed Matter **27**, 166002 (2015).

[26] T. Sato, T. Masuda, and K. Uchinokura, Physica B: Condensed Matter **329-333**, 880 (2003), proceedings of the 23rd International Conference on Low Temperature Physics.

[27] S. Miyahara and N. Furukawa, Journal of the Physical Society of Japan **80**, 073708 (2011), https://doi.org/10.1143/JPSJ.80.073708.

[28] J. Romhányi and K. Penc, Phys. Rev. B **86**, 174428 (2012).

[29] J. Jeong, M. D. Le, P. Bourges, S. Petit, S. Furukawa, S.-A. Kim, S. Lee, S.-W. Cheong, and J.-G. Park, Phys. Rev. Lett. **113**, 107202 (2014).

[30] O. P. Vajk, M. Kenzelmann, J. W. Lynn, S. B. Kim, and S.-W. Cheong, Journal of Applied Physics **99**, 08E301 (2006).

[31] I. V. Solovyev, Phys. Rev. B **91**, 224423 (2015).

[32] P. Toledano, D. D. Khalyavin, and L. C. Chapon, Phys. Rev. B **84**, 094421 (2011).